Monatshefte für Chemie - Chemical Monthly (2020) 151:11–23
https://doi.org/10.1007/s00706-019-02537-w

ORIGINAL PAPER

Substituent effects on stability, MEP, NBO analysis, and reactivity of 2,2,9,9-tetrahalosilacyclonona-3,5,7-trienylidenes, at density functional theory

Maryam Koohi[1,2] · **Hajieh Bastami**[3]

Received: 27 August 2019 / Accepted: 11 December 2019 / Published online: 6 January 2020

Abstract

Cyclonona-3,5,7-trienylidene appears as boat-shaped transition state for having a negative force constant, while its singlet state exhibits less stability than the corresponding triplet state. Succeeding the quest for the largest unsaturated stable carbene-like species, theoretical investigations coupled with suitable isodesmic reactions are used to examine the effects of α,α'-tetrahalo groups on the thermodynamic along with kinetic viabilities of nine-membered cyclic silylenes. All the singlet and triplet silylenes appear as boat-shaped minima for having positive force constants on their potential energy surfaces and singlet states emerge as ground state, exhibiting more stability than their corresponding triplet states. The order of stability estimated by singlet (S)–triplet (T) energy separation ($\Delta E_{S-T} = E_T - E_S$) emerges as α,α'-tetrahydrocarbene < α,α'-tetrahydrosilylene < α,α'-tetrafluorosilylene < α,α'-tetraiodosilylene < α,α'-tetrachlorosilylene < α,α'-tetrabromosilylene. This research specifies band gap ($\Delta E_{HOMO-LUMO}$) of scrutinized silylenes with this order. Hence, singlet 2,2,9,9-tetrabromosilacyclonona-3,5,7-trienylidene exists as the most stable species. From both thermodynamic and kinetic points of view, this species is more stable than synthesized silylene by Kira. It shows the highest heat of dehydrogenation through isodesmic reaction. The NBO analysis provides significant evidences for the stability of it through positive hyperconjugation, negative hyperconjugation, as well as mesomeric effects.

Graphic abstract

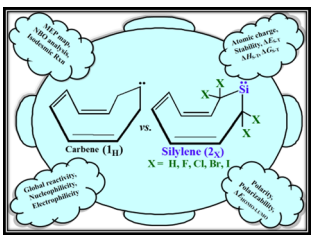

Keywords Silylene · Stability · Carbene-like species · Isodesmic reaction

Electronic supplementary material The online version of this article (https://doi.org/10.1007/s00706-019-02537-w) contains supplementary material, which is available to authorized users.

✉ Hajieh Bastami
bastami@shariaty.ac.ir; Hbastami@tvu.ac.ir

[1] Young Researchers and Elites Club, North Tehran Branch, Islamic Azad University, Tehran, Iran

[2] Department of Chemistry, North Tehran Branch, Islamic Azad University, Tehran, Iran

[3] Technical and Vocational, University of Tehran, Dr. Shariaty College, 16851-18918 Tehran, Iran

Introduction

Silylenes (R_2Si:) as one of the heavier analogs of carbenes (R_2C:) are key intermediates in numerous thermal and photochemical reactions of organosilicon compounds [1, 2]. Contrary to carbon, silicon has low ability to form hybrid orbitals and a typical silicon prefers $(3s)^2(3p)^2$ valence electronic configuration which leads to the carbene-like singlet ground state [1, 2]. This is due to the difference in

geometrical sizes of the ns and np orbitals when $n > 2$. While methylene (H_2C:) has a triplet ground state with a ΔE_{S-T} of − 37.6 kJ/mol, the ground state of silylene (H_2Si:) is a singlet that lies 79–96 kJ/mol lower than its corresponding triplet state. Silylenes show ambiphilic character because of the presence of an occupied s-orbital and vacant p-orbital that makes silylenes react either as an electrophile or nucleophile. Henceforth, in a silylene, two electrons occupy 3s orbital leading to a singlet ground state (Fig. 1).

There are many ways to enhance the nucleophilicity of silylenes such as using a Lewis base [3]. The σ-donation ability and high nucleophilicity of silylenes [4, 5] make them promising compounds in H-abstraction reactions, dimerization, and transition metal bridging ligands [6, 7]. While a broad assortment of N-heterocyclic silylene-transition metal complexes [8–11] and acyclic silylene ligands [12, 13] have been reported, the carbocyclic silylene ligands are less considered [14]. To suggest a sufficient stable silylene for isolation, the thermodynamic and kinetic characterization of the reactive vacant p-orbital is essential (the lone pair is inert by reason of its high s-character) [15, 16]. The synthesis of the first stable five-membered cyclic silylene **I** (Scheme 1) in 1994 by Denk et al. was indebted to both the electron donating from the adjacent nitrogens (thermodynamic stabilization) and the steric hindrance provided by *t*-Bu groups (kinetic stabilization) [17]. Consequently, silylenes **II**–**VI** were synthesized (Scheme 2) [18–22].

In our previous works, one of us studied carbenic derivatives of $\mathbf{1_H}$ containing α-cyclopropylcyclonona-3,5,7-trienylidenes which are substituted with $\acute{\alpha}$-NMe, PMe, O, S, CH_2, cyclopropyl, and CMe_2 groups ($\mathbf{1_{X\acute{\alpha}}}$) (Scheme 3) [23–25].

Interestingly, $\mathbf{1_H}$ appears as a transition state 17.1 kJ/mol less stable than its substituted analogous as the global minima [23–25]. These studies called for further quantitative investigations on the stabilizing effects of other hetero atoms, such as halogens. Up-to-date, nothing has been done to study the substituent effect on the largest non-planar unsaturated cyclic silylenes with $C_8H_6X_4Si$: molecular formula, $\mathbf{2}_X$ (where X = H, F, Cl, Br, and I) via experimental and theoretical methods (Fig. 2). Here, a brief comparison is also made among these results with those of some stable synthesized silylenes **I**, **V**, and **VII** (Scheme 4) [18–22].

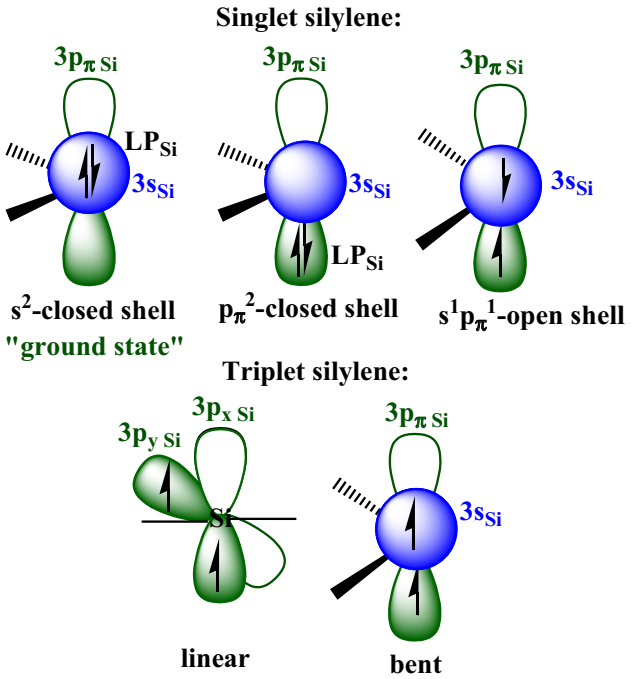

Fig. 1 Possible electronic configurations and orbitals of singlet and triplet silylenes

Results and discussion

Following our quest for stable cyclic compounds bearing divalent group 14 atoms, here, density functional theory (DFT) calculations are employed to form a systematic investigation on the effects of halogen substitutions on the atomic charge distribution, thermodynamic stability as a measure of ΔE_{S-T}, polarity, polarizability, kinetic stability as a measure of $\Delta E_{HOMO-LUMO}$, and NBO analysis of scrutinized species (Fig. 2). In each series of calculations, the results are made through comparison to the parent carbene $\mathbf{1_H}$. To verify the validity of widely accepted B3LYP method for the

Scheme 1

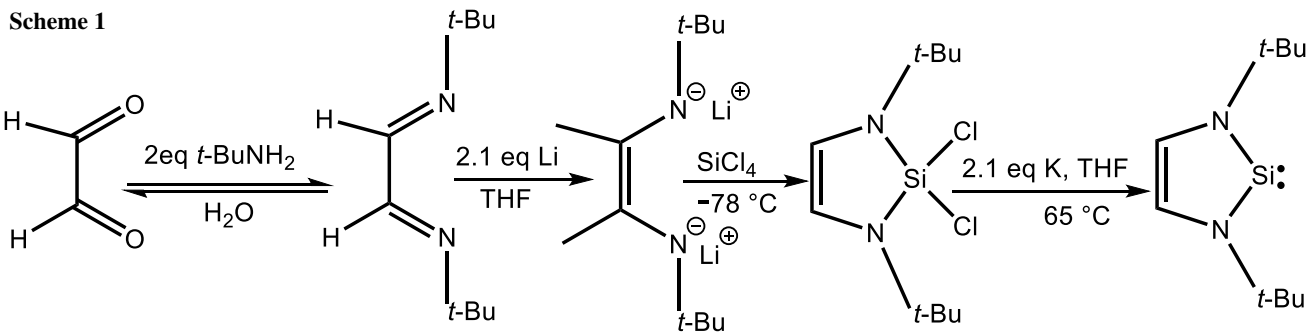

Scheme 2

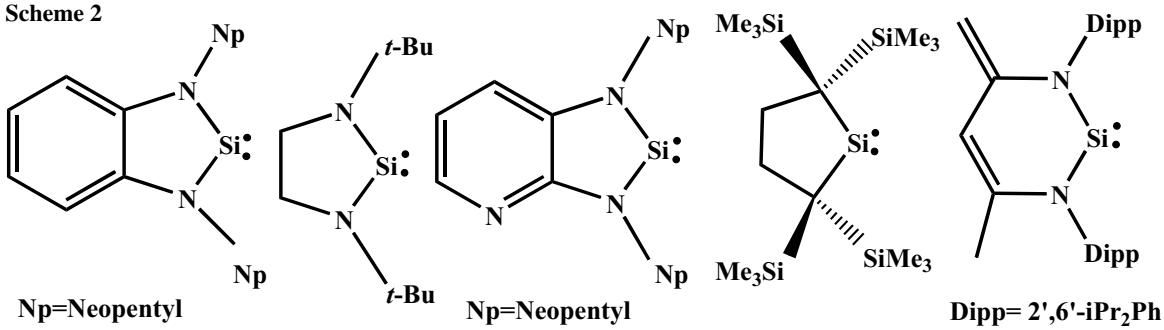

II	III	IV	V	VI
Lappert	West	Heinicke	Kira	Driess
1995	1996	1998	1999	2006

Scheme 3

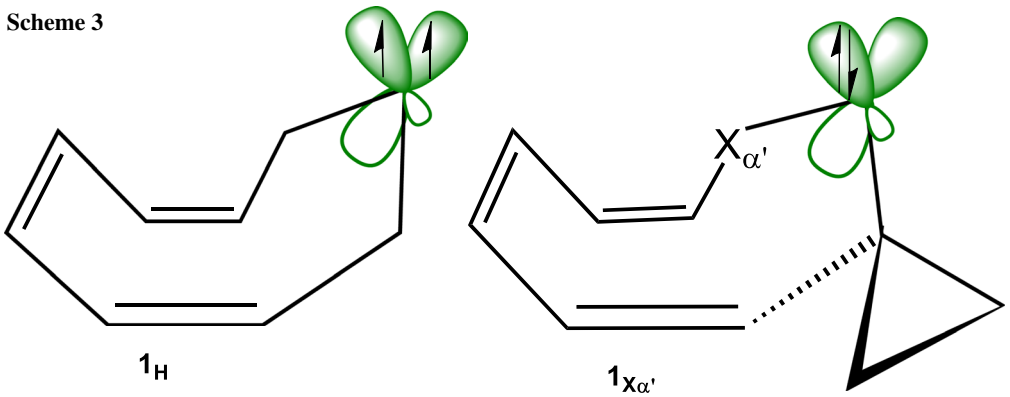

($X_{\alpha'}$ = NMe, PMe, O, S, cyclopropyl, CMe_2, and CH_2)

Triplet Transition State Singlet Minima

optimizations and energy computations, all molecules are re-optimized with more accurate but time-consuming M06-2X method. The differences among the results obtained from the two methods are not significant. Henceforth, the remaining calculations are concentrated on B3LYP.

Substituent effects on charge, ΔE_{S-T}, and polarity

Owing to the intrinsic properties of scrutinized silylenes, their triplet structures show less atomic charge distribution on Si:, C_2 (C_α), C_9 ($C_{\alpha'}$) than those of their corresponding singlet states, at B3LYP/AUG-cc-pVTZ (Table 1).

Replacement of the carbene (in our previous work) [23–25] with silylene in the present research leads to an increase in the p-character of C–Si compared to C–C bond [26]. In the present study, a decrease in the C–D–C angle; D being the divalent, carbene-like atom (Â/degree) is observed from 121.19° for C-D-C angle ('D' refers to the 'divalent' atom) in $\mathbf{1_{H-S}}$ carbene to 97.06° for the corresponding C–Si–C in $\mathbf{2_{H-S}}$ silylene (Table S1). Substituting of the carbene with silylene leads to an increase in the bond lengths X_2C–Si: compared to X_2C–C: bond. Also, X–C_2 (C_α), and X–C_9 ($C_{\alpha'}$) bond lengths seem linearly proportional to the size of the substitution element (X = H, F, Cl, Br, and I). The T structures show larger C_9–Si–C_2 or $C_{\alpha'}$–Si–C_α angles and less Si–C_2 (C_α), Si–C_9 ($C_{\alpha'}$) bond lengths than those of their corresponding S states, at B3LYP/LANL2DZ-6-311 + G* level (Table S1).

Substitution of CH_2–C:–CH_2 with CH_2–Si:–CH_2 in $\mathbf{1_H}$ alters its status from an unstable transition state to rather stable minimum for showing no negative force constant (Table 2).

Replacement of α,α′-CH_2 with CF_2, CCl_2, CBr_2, and CI_2 in $\mathbf{2_H}$ alter their status from an unstable triplet transition state to rather stable singlet minima (Table 2). These singlet silylenes emerge as ground states, showing more stability than their corresponding triplet states. The overall stability order of the calculated and synthesized silylenes (**I**, **V**, and **VII**) based on their ΔE_{S-T} values is: $\mathbf{VII > I > 2_{Br} > 2_{Cl} > 2_I > V > 2_F > 2_H}$. Beyond such a high stability lays the mesomeric

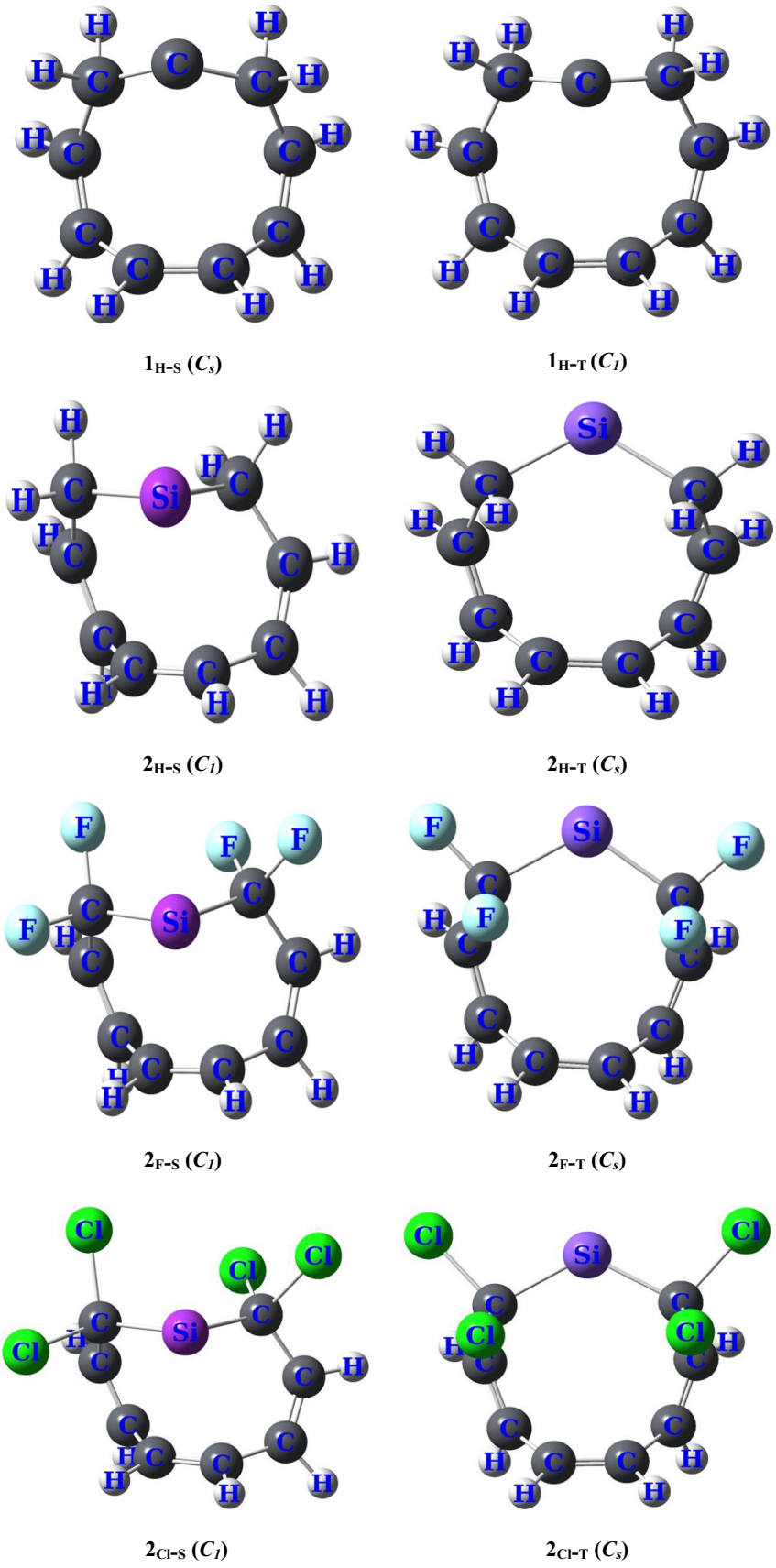

Fig. 2 The optimized singlet carbene ($\mathbf{1_{H\text{-}S}}$) and singlet silylenes ($\mathbf{2_{H\text{-}S}}$, $\mathbf{2_{F\text{-}S}}$, $\mathbf{2_{Cl\text{-}S}}$, $\mathbf{2_{Br\text{-}S}}$, $\mathbf{2_{I\text{-}S}}$) are compared and contrasted to their corresponding triplet states ($\mathbf{1_{H\text{-}T}}$, $\mathbf{2_{H\text{-}T}}$, $\mathbf{2_{F\text{-}T}}$, $\mathbf{2_{Cl\text{-}T}}$, $\mathbf{2_{Br\text{-}T}}$, $\mathbf{2_{I\text{-}T}}$) along with their corresponding symmetries, at B3LYP/AUG-cc-pVTZ level

Fig. 2 (continued)

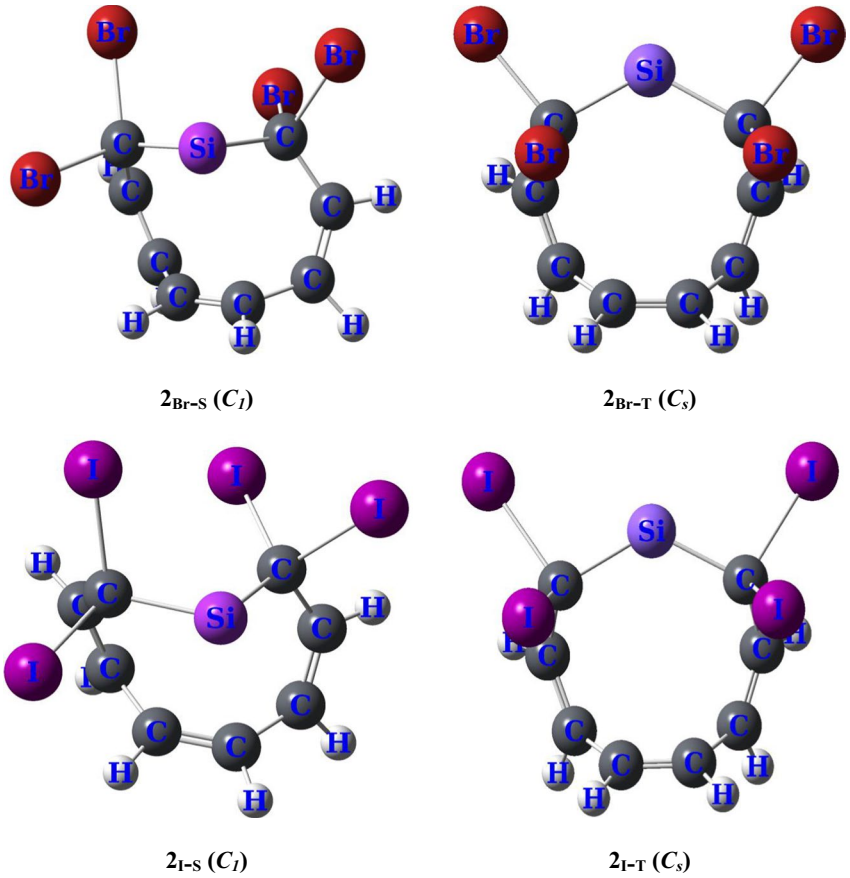

Scheme 4

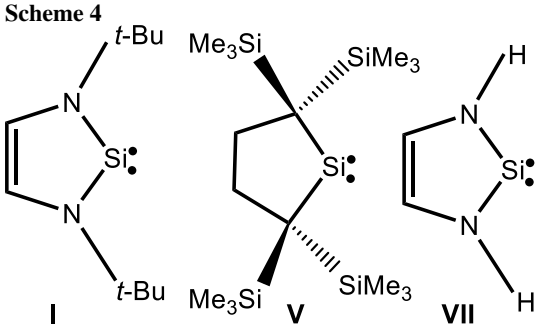

effects of non-planar cyclic $\mathbf{2_{Br-S}}$, $\mathbf{2_{Cl-S}}$, and $\mathbf{2_{I-S}}$ compared to $\mathbf{VII\text{-}_S}$, and $\mathbf{I}_S$ which are cyclic, planar, continuously conjugated and obeys Hückel rule of 4n + 2 (Fig. 3).

Moreover, $\mathbf{2_{Br}\text{-}_S}$, $\mathbf{2_{Cl}\text{-}_S}$, and $\mathbf{2_{I}\text{-}_S}$ show the higher stability than $\mathbf{V\text{-}_S}$. The larger the substituents (—$SiMe_3$) have the smaller stabilizing effect on carbene-like atom than the Cl, Br, and I heteroatoms. It was found that B3LYP is the most efficient method to use in performing calculations of carbene-like atoms [23–25]. In Table 2, it can be seen that after full optimization of scrutinized species, the spin contamination parameters $< S^2 >$ for singlet closed shell states are zero, while the spin eigenvalues are relatively closer together for diradical triplet states (more than 2.00), indicating that those wave functions were contaminated with higher spin states. Fascinatingly, our triplet parent carbene shows higher S^2 than its corresponding silylenic analogous, and the S^2 value for triplet silylenes increases as a function of the ring size and size of substituted group $\mathbf{VII\text{-}_T < I\text{-}_T < V\text{-}_T < 2_{H}\text{-}_T < 2_{F}\text{-}_T < 2_{Cl}\text{-}_T < 2_{Br}\text{-}_T < 2_{I}\text{-}_T}$ and it increases as the steric effect increases.

The zero-point (ZP) correction and zero-point vibrational energy (ZPVE) decrease in going from singlet silylenes to their corresponding triplet states, and in going from $\mathbf{2_H}$ to $\mathbf{2_I}$. In contrast, the stability of the synthesized species decreases in going from the cyclic-saturated **V** to cyclic-unsaturated diaminosilylenes **I**, and **VII**, respectively, that both become more stable in the presence of heteroatoms.

We have probed changes of enthalpy (ΔH_{S-T}) and Gibbs free energy (ΔG_{S-T}) which confirm the higher stability of singlet silylenes (Table S2). As anticipated, ΔH_{S-T} and ΔG_{S-T} trends for silylenes appear the same as that of $\Delta E_{S\text{-}T}$, at B3LYP/LANL2DZ-6-311 ++G** level: $\mathbf{VII > I > 2_{Br} > 2_{Cl} > 2_I > V > 2_F > 2_H}$. Simultaneously, among our silylenes, $\mathbf{2_{Br}\text{-}_S}$ and $\mathbf{2_{Br}\text{-}_T}$ exhibit the highest changes of enthalpy ($\Delta H_{S-T} = 170.63$ kJ/mol) and free energy ($\Delta G_{S-T} = 165.61$ kJ/mol) (Table S2). These results are consistent with their relatively high stability difference

Table 1 The NBO atomic charge distribution on divalent, carbene-like atom (D), C_2 (C_α), C_9 ($C_{\alpha'}$), X_1, and X_2 atoms calculated for unsubstituted singlet, and triplet carbenes ($\mathbf{1_{H\text{-}S}}$, and $\mathbf{1_{H\text{-}T}}$) and their corresponding tetrahalosilylenic analogous ($\mathbf{2_{H\text{-}S}}$, $\mathbf{2_{H\text{-}T}}$, $\mathbf{2_{F\text{-}S}}$, $\mathbf{2_{F\text{-}T}}$, $\mathbf{2_{Cl\text{-}S}}$, $\mathbf{2_{Cl\text{-}T}}$, $\mathbf{2_{Br\text{-}S}}$, $\mathbf{2_{Br\text{-}T}}$, $\mathbf{2_{I\text{-}S}}$, and $\mathbf{2_{I\text{-}T}}$, respectively), at (U)B3LYP/AUG-cc-pVTZ level

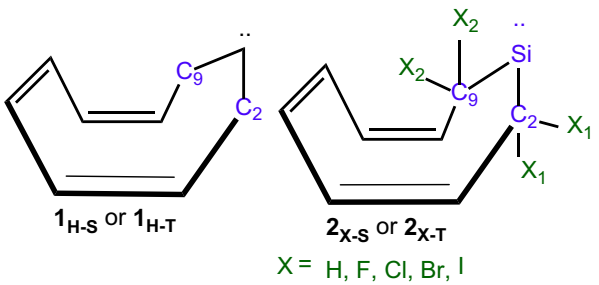

Structures	D	C_2 (C_α)	C_9 ($C_{\alpha'}$)	X_1	X_2
$\mathbf{1_{H\text{-}S}}$	0.600	−0.864	−0.783	0.153	0.211
$\mathbf{1_{H\text{-}T}}$	0.693	−0.900	−0.809	0.181	0.232
$\mathbf{2_{H\text{-}S}}$	0.670	−0.856	−0.893	0.235	0.211
$\mathbf{2_{H\text{-}T}}$	0.522	−0.845	−0.845	0.252	0.230
$\mathbf{2_{F\text{-}S}}$	0.713	−0.078	−0.112	−0.229	−0.211
$\mathbf{2_{F\text{-}T}}$	0.560	−0.008	−0.008	−0.215	−0.187
$\mathbf{2_{Cl\text{-}S}}$	0.915	−0.881	−0.852	0.050	0.031
$\mathbf{2_{Cl\text{-}T}}$	0.805	−0.813	−0.813	0.057	0.041
$\mathbf{2_{Br\text{-}S}}$	0.943	−1.019	−1.001	0.122	0.082
$\mathbf{2_{Br\text{-}T}}$	0.876	−0.990	−0.990	0.105	0.105
$\mathbf{2_{I\text{-}S}}$	0.616	−0.966	−0.946	0.210	0.194
$\mathbf{2_{I\text{-}T}}$	0.584	−0.708	−0.708	0.125	0.058

(ΔE_{S-T} = 172.42 kJ/mol), and NBO charge distribution on Si, C_2 (C_α), C_9 ($C_{\alpha'}$) atoms.

Paired electrons on divalent centers lead to higher dipole moments (μ) in singlet structures ($\mathbf{1_{H\text{-}S}}$ – $\mathbf{2_{I\text{-}S}}$, and $\mathbf{V\text{-}_S}$) than their corresponding triplet states ($\mathbf{1_{H\text{-}T}}$ – $\mathbf{2_{I\text{-}T}}$, and $\mathbf{V\text{-}_T}$) where the non-bonding electrons of Si atom in singlet states are paired and located in the σ-orbital which is orthogonal to π-system. While, lower μ values of $\mathbf{I\text{-}_S}$ and $\mathbf{VII\text{-}_S}$ with respect to their corresponding triplets and studied singlets ($\mathbf{1_{H\text{-}S}}$–$\mathbf{2_{I\text{-}S}}$) show that the non-bonding electrons of divalent silicon in formers are paired in the π-orbital which participate to ring current of π-system. Also, an increase of μ (in Debye) is observed from 2.18 in $\mathbf{1_{H\text{-}S}}$ and 1.75 in $\mathbf{2_{H\text{-}S}}$ to 6.30 in $\mathbf{2_{F\text{-}S}}$ vs. 0.43 in $\mathbf{1_{H\text{-}T}}$, 0.57 in $\mathbf{2_{H\text{-}T}}$, and 4.00 Debye in $\mathbf{2_{F\text{-}T}}$ (Table 2). Evidently, polarity for singlets increases as electronegativity of substitutions increases and polarizabilities (α_{xx}, α_{yy}, α_{zz}, and $<\alpha>$) increase as a function of the substitution size of halogen and carbene-like atoms, and it decreases as μ increases. Our triplet carbene-like atoms show higher α_{xx}, α_{yy}, α_{zz}, and $<\alpha>$ than their corresponding singlet structures. For instance, $\mathbf{2_{I\text{-}T}}$ (218.82 a.u.) displays a higher polarizability than $\mathbf{2_{I\text{-}S}}$ (206.44 a.u.) compared to parent triplet and singlet carbenes (107.79, and 106.32 a.u., respectively) (Table S3).

Substituent effects on heat of hydrogenation of HOMO-LUMO gap, MEP map, reactivity, and NBO analysis

It is well known that the HOMO–LUMO energy gap is associated with the chemical stability to electronic excitation; the larger $\Delta E_{HOMO-LUMO}$, the more chemically stable compound. Moreover, the trend of kinetic stability based on $\Delta E_{HOMO-LUMO}$ is: $\mathbf{VII > I > 2_{Br} > 2_{Cl} > 2_I > V > 2_F > 2_H > 1_H}$, and leads to the stability enhancing against electronic excitations (Table 3).

This means that the electron in $\mathbf{2_{Br}}$ is tighter to excite from the highest occupied molecular orbital (HOMO) to the lowest unoccupied molecular orbital (LUMO) than in the synthesized silylene **V** (412.61 vs. 351.33 kJ/mol). As anticipated, this trend is the same as that of ΔH_{S-T}, ΔG_{S-T}, and ΔE_{S-T}.

Molecular electrostatic potential (MEP) map is a useful feature to examine the reactivity given that an approaching electrophile will be drawn into negative areas (the electron distribution in where effect is dominant). The importance of MEP lies in the fact that it simultaneously displays molecular size, shape as well as positive, negative, and neutral electrostatic potential regions in terms of color grading, and is very useful in research of molecular structure with its physiochemical property relationship [27]. Interestingly, the MEP maps are consistent with their point groups, atomic charge distribution on carbene-like atoms, C_2 (C_α), C_9 ($C_{\alpha'}$), substitution atoms, and polarities (Fig. 2 and S1). For instance, the most positive charge is predicted for $\mathbf{2_{Br\text{-}S}}$ with the highest blue-colored cloud on its silicon atom. Simultaneously, the most negative charge is demonstrated for $\mathbf{2_{Br\text{-}S}}$ with the highest red colored electron cloud on its C_2 (C_α), C_9 ($C_{\alpha'}$) atoms. In this study, every S and T speciesshows the highest difference between size, shape, along with positive and negative electrostatic potential regions in terms of color grading, because of having the highest difference between its substitution effects and polarizability (Fig. S1 and Table S3). The MEP map can also be utilized to define the nature of a molecule chemical bond and the electronegativity difference is a central causal factor in this definition. When silicon, hydrogen, and/or halogen atoms with carbon atom are to form bond, their bond will be expected to be polar covalent. Since hydrogen, halogen, and carbon atoms have higher electronegativity than silicon atom, the former will share the binding electrons with Si, but the binding electrons will be pulled closer to the more electronegative atoms, forming dipoles within the carbene-like containing molecule. We expect these bonds to be polar covalent (partly ionic),

Table 2 The calculated total energy (E_{tot}), $\Delta E_{S\text{-}T}$, spin contamination parameter $<S^2>$, zero-point (ZP) correction, ZP vibrational energy (ZPVE) and dipole moment (μ) for studied carbene, and silylenes *vs.* the synthesized silylenes **I**, **V**, and **VII** (Scheme 4)

Species	$E_{tot}^{1,(2)}$/Hartree	$\Delta E_{S\text{-}T}^{1,(2)}$/kJ mol^{-1}	$<S^2>^3$	ZP correction[3]/Hartree	ZPVE[3]/kJ mol^{-1}	μ[1]/Debye
$\mathbf{1_{H\text{-}S}}$	−348.860724, (−345.704825)	−22.78, (−10.95)	0.0000	0.194072	509.04	2.18
$\mathbf{1_{H\text{-}T}}$	−348.867724, (−345.708999)		2.0074	0.194099	510.29	0.43
$\mathbf{2_{H\text{-}S}}$	−600.102782, (−600.096185)	115.49, (107.55)	0.0000	0.155082	405.79	1.75
$\mathbf{2_{H\text{-}T}}$	−600.058318, (−600.055184)		2.0040	0.154340	404.79	0.57
$\mathbf{2_{F\text{-}S}}$	−997.097388, (−997.031714)	142.62, (150.06)	0.0000	0.122205	320.52	6.30
$\mathbf{2_{F\text{-}T}}$	−997.043247, (−996.974511)		2.0058	0.121831	319.56	4.00
$\mathbf{2_{Cl\text{-}S}}$	−2438.499181, (−2438.45241)	160.72, (168.54)	0.0000	0.116183	304.72	5.31
$\mathbf{2_{Cl\text{-}T}}$	−2438.438448, (−2438.38815)		2.0065	0.115496	302.92	3.60
$\mathbf{2_{Br\text{-}S}}$	−10884.645942, (−10884.995413)	172.42, (198.63)	0.0000	0.114386	299.99	4.42
$\mathbf{2_{Br\text{-}T}}$	−10884.580894, (−10884.919684)		2.0067	0.113435	297.53	3.26
$\mathbf{2_{I\text{-}S}}$	−643.342144, (−641.269648)	156.08, (163.94)	0.0000	0.112177	294.23	3.99
$\mathbf{2_{I\text{-}T}}$	−643.287144, (−641.207145)		2.0072	0.111227	291.72	2.72
$\mathbf{I_{S}}$	−792.2723674, (−792.274367)	224.63, (230.28)	0.0000	0.290173	761.09	1.28
$\mathbf{I_{T}}$	−792.1867261, (−792.186568)		2.0020	0.288082	755.62	3.34
$\mathbf{V_{S}}$	−2081.630027, (−2081.634027)	138.48, (149.56)	0.0000	0.519409	1362.39	1.15
$\mathbf{V_{T}}$	−2081.577227, (−2081.577007)		2.0044	0.519162	1361.72	0.90
$\mathbf{VII_{S}}$	−477.7155363, (−477.712536)	258.49, (251.09)	0.0000	0.066765	175.10	1.61
$\mathbf{VII_{T}}$	−477.6169938, (−477.616804)		2.0024	0.064560	169.33	3.92

[1]At the B3LYP/AUG-cc-pVTZ, and UB3LYP/AUG-cc-pVTZ for singlet, and triplets, respectively

[2]At the M06-2X/AUG-cc-pVDZ, and UM06-2X/AUG-cc-pVDZ (values in parenthesis) for singlet, and triplet states, respectively

[3]At the B3LYP/LANL2DZ-6-311++G**, and UB3LYP/LANL2DZ-6-311++G** for singlet, and triplet states, respectively

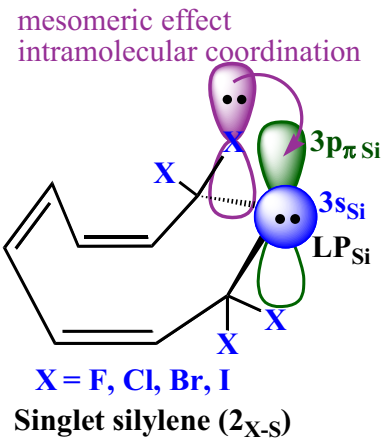

Fig. 3 Substituent effects of halogen atoms on singlet silacyclonona-3,5,7-trienylidenes

because the difference in electronegativity is between 0.4 eV and 2.0 eV on Pauling's scale.

As said previously, the extremely high reactivity of a silylene is due to its unoccupied $3p_\pi$ orbital, since six valence electrons are less than the eight electrons needed by the octet rule, and its lone pair is predicted to be inert owing to its high s-character [28]. Henceforth, to classify the reactivity of scrutinized silylenes, their nucleophilicity index (N), global electrophilicity (ω), chemical potential (μ), global hardness (η), electronegativity (χ), global softness (S), and maximum electronic charge (ΔN_{max}) are evaluated using appropriate indices (Table S4). N values show conspicuous correlations with the corresponding MEP maps for calculated silylenes (Table S4 and Fig. S1). These are consistent with the energy along with pictorial sizes of the frontier molecular orbitals (Fig. S2). The $\mathbf{2_{F\text{-}S}}$ has the highest absolute values of E_{HOMO} and E_{LUMO}. Due to the intrinsic properties of fluorine atom, $\mathbf{2_{F\text{-}S}}$ has the lowest N, the highest ω as well as the highest χ, while its unsubstituted silylenic and carbenic analogous ($\mathbf{2_{H\text{-}S}}$ and $\mathbf{1_{H\text{-}S}}$) show an inverse relationship. $\mathbf{1_{H\text{-}S}}$, and $\mathbf{2_{H\text{-}S}}$ silylenes show higher N than the synthesized silylenes **I**, **V**, and **VII**. Our halogenated silylenes show higher ωthan the synthesized silylenes **I**, **V**, and **VII**. Also, $\mathbf{1_{H\text{-}S}}$ is the most reactive carbene-like species, as dictated by the maximum N, minimum, along with maximum S. Interestingly, $\mathbf{2_{Br\text{-}S}}$ is the least reactive structure with the maximum and all calculated silylenes have more η and less S than the synthesized silylene **V** (Table S4). All calculated and synthesized species have positive values of ΔN_{max} with the range of 0.65–1.12 eV (for the synthesized silylene **I** and $\mathbf{2_{F\text{-}S}}$, respectively), and, hence, act as electron acceptors from their environment.

Table 3 The calculated frontier molecular orbital energy (E_{HOMO}, E_{LUMO}), and $\Delta E_{HOMO\text{-}LUMO}$ for the scrutinized structures compared to the synthesized silylenes **I**, **V**, and **VII** (Scheme 4), at B3LYP/LANL2DZ-6-311 ++G** level

Structures	E_{HOMO}/Hartree	E_{LUMO}/Hartree	$\Delta E_{HOMO\text{-}LUMO}$/kJ mol^{-1}	$\Delta E_{HOMO\text{-}LUMO}$/eV
$\mathbf{1_{H\text{-}S}}$	−0.17709	−0.05629	316.84	3.29
$\mathbf{2_{H\text{-}S}}$	−0.18720	−0.03985	386.48	4.01
$\mathbf{2_{F\text{-}S}}$	−0.24189	−0.09224	392.54	4.07
$\mathbf{2_{Cl\text{-}S}}$	−0.23828	−0.08300	407.30	4.23
$\mathbf{2_{Br\text{-}S}}$	−0.23909	−0.08179	412.61	4.28
$\mathbf{2_{I\text{-}S}}$	−0.22723	−0.07508	399.06	4.14
I	−0.18932	−0.02509	430.75	4.47
V	−0.20411	−0.07017	351.33	3.64
VII	−0.20084	−0.02868	451.57	4.68
TCNE[1]	−0.34764	−0.1951	400.11	4.15

[1] *TCNE* tetracyanoethylene as a reference

To clarify the role of substituent effect in stability of silylenes, one may refer to the second-order interactions of donor (Lewis-type) and acceptor (non-Lewis-type) NBO orbitals that point to the extent of substituent effect in silylenes. NBO analysis is originally recognized as a way of quantifying resonance structure contributions to molecules and is carried out by surveying all probable interactions between electron donor and electron acceptor NBO orbitals, along with estimating their energetic importance of second-order perturbation theory [29–32]. Therefore, some of valence data including occupancy, directionality, and hybridization resulting of NBO calculation on stable $\mathbf{2_{Br\text{-}S}}$ silylene, at B3LYP/6-311 ++G**, are given in Table 4.

Table 4 The bond orbital, occupancy, coefficients, and hybrids corresponding to the intramolecular bonds in stable $\mathbf{2_{Br\text{-}S}}$ species, at B3LYP/LANL2DZ-6-311 ++G** level

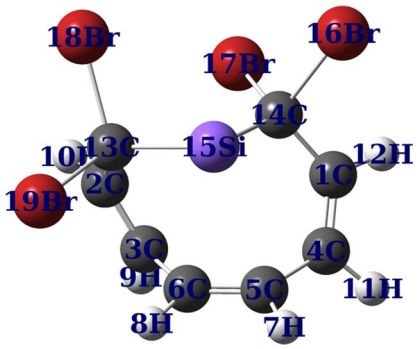

Bond (A-B)	Occup.	ED_A/ %	ED_B/ %	NBO	*s*/ %	*p*/ %
$\sigma_{C13\text{-}Si15}$	1.94053	80.90	19.10	$*0.8994sp^{2.04} + *0.4371sp^{7.08}$	32.95 ($_{C13}$), 12.37 ($_{Si15}$)	67.05 ($_{C13}$), 87.63 ($_{Si15}$)
$\sigma_{C13\text{-}Br18}$	1.99571	50.00	50.00	$0.7071*sp^{5.23} + *0.7071sp^{6.83}$	16.06 ($_{C13}$), 12.77 ($_{Br18}$)	83.94 ($_{C13}$), 87.23 ($_{Br18}$)
$\sigma_{C13\text{-}Br19}$	1.96857	49.47	50.53	$0.7034*sp^{5.09} + 0.7108*sp^{7.63}$	16.41 ($_{C13}$), 11.59 ($_{Br19}$)	83.59 ($_{C13}$), 88.41 ($_{Br19}$)
$\sigma_{C14\text{-}Si15}$	1.95051	80.77	19.23	$0.8987*sp^{1.83} + 0.4385*sp^{8.10}$	35.31 ($_{C14}$), 10.99 ($_{Si15}$)	64.69 ($_{C14}$), 89.01 ($_{Si15}$)
$\sigma_{C14\text{-}Br16}$	1.96422	48.26	51.74	$0.6947*sp^{6.15}\ 0.7193 + *sp^{7.66}$	13.99 ($_{C14}$), 11.54 ($_{Br16}$)	86.01 ($_{C14}$), 88.46 ($_{Br16}$)
$\sigma_{C14\text{-}Br17}$	1.99459	50.13	49.87	$0.7080*sp^{4.81} + 0.7062*sp^{7.57}$	17.22 ($_{C14}$), 11.67 ($_{Br17}$)	82.78 ($_{C14}$), 88.33 ($_{Br17}$)
LP_{Si15}	1.92854			$sp^{0.28}$	77.98	22.02
LP_{Br16}	1.99005			$sp^{0.21}$	82.97	17.03
LP_{Br17}	1.98912			$sp^{0.15}$	87.11	12.89
LP_{Br18}	1.98841			$sp^{0.18}$	84.61	15.39
LP_{Br19}	1.98973			$sp^{0.23}$	81.10	18.90

The intermolecular interaction is formed by the orbital overlap between C-Si, C–Br, and the corresponding anti-bonding orbital which results in an intermolecular charge transfer (ICT) from a Lewis valence orbital as donor, with a decreasing of its occupancy, to a non-Lewis orbital as acceptor. The first two columns of this table give the type of orbital and occupancy among 1.92854 and 1.99571 electrons. Analysis of occupancy number provides useful information about the formation of singlet and/or triplet silylenes. For instance, $\sigma_{C13\text{-}Br18}$ and $\sigma_{C14\text{-}Br17}$ bonding orbitals with the highest occupancies 1.99571 and 1.99459 electrons have 50.00% C_{13} and 50.13% C_{14} characters in a $sp^{5.23}$ and $sp^{4.81}$ hybrids and have 50.00% Br_{18} and 49.87% Br_{17} characters in a $sp^{6.83}$ and $sp^{7.57}$ hybrids, respectively. The $sp^{5.23}$ hybrid on C_{13} has 16.06% s-character and 83.94% p-character, while the $sp^{6.83}$ hybrid on Br_{18} has 12.77% s-character and 87.23% p-character, respectively with polarization coefficient of 0.7071. The magnitude of this coefficient indicates the significance of the two hybrids in bond formation. While, $\sigma_{C13\text{-}Si15}$, and $\sigma_{C14\text{-}Si15}$ bonding orbitals show that their silicon centers have a lesser percentage of NBOs (19.10 and 19.23%, respectively) and give a lesser polarization coefficients (0.4371 and 0.4385, respectively) than the other bonding bonds, because silicon atom has a lower electronegativity than bromine and carbon atoms (1.90 vs. 2.96 and 2.55). Also, occupancy number for lone pair on Si (1.92854) of $\mathbf{2_{Br\text{-}S}}$ shows high s-character (77.98%) indicating the paired electrons in s-orbital. The calculated second-order interaction energies ($E^{(2)}$) among the orbital's donors–acceptor in stable $\mathbf{2_{Br\text{-}S}}$ silylene are shown in Table S4. Overall, donation of $\sigma_{C\alpha\text{-}Br}$ including $\sigma_{C13\text{-}Br18}$, $\sigma_{C13\text{-}Br19}$, $\sigma_{C14\text{-}Br16}$, and $\sigma_{C14\text{-}Br17}$ to LP^*_{Si} ($3p_{\pi\ Si}$) through positive hyperconjugation on one side and donation of lone pairs on bromine atom to unoccupied orbital of silicon center via mesomeric effect on the other side are totally more than donation of lone pairs on silicon center (σ^2_{Si}) to the anti-bonding orbitals of $\sigma^*_{C\alpha\text{-}Br}$ (that is $LP_{Si15} \rightarrow \sigma^*_{C13\text{-}Br19}$, $LP_{Si15} \rightarrow \sigma^*_{C14\text{-}Br17}$, $LP_{Si15} \rightarrow \sigma^*_{C14\text{-}Br16}$, and $LP_{Si15} \rightarrow \sigma^*_{C13\text{-}Br18}$) through negative hyperconjugation (Table S5 and Fig. 4).

Clearly, higher interaction among $\sigma_{C\alpha\text{-}Br}$ as donor and $3p_{\pi\ Si}$ as acceptor via positive hyperconjugation on one side and so effective interaction between $\mathbf{LP_{Br}}$ as donor with $3p_{\pi\ Si}$ as acceptor through mesomeric effect on the other side leads to the elongation of the acceptor. All these intramolecular interactions confirm the higher stability and lower

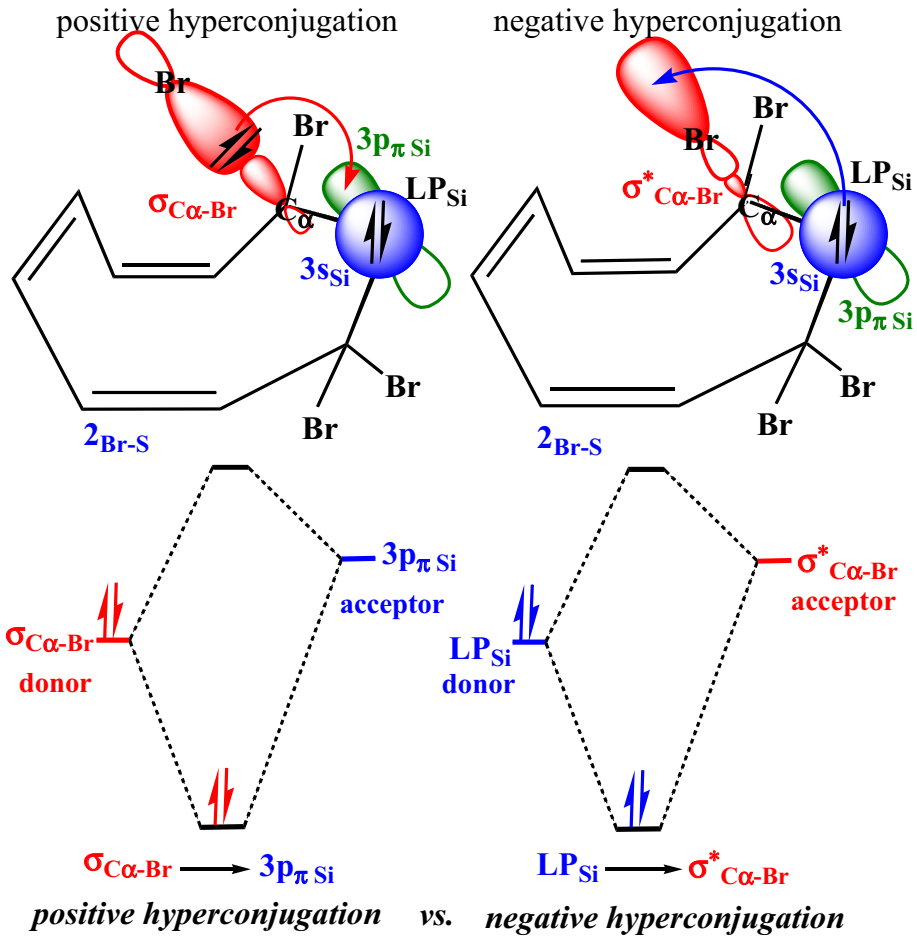

Fig. 4 Positive vs. negative hyperconjugations and their corresponding perturbation orbital diagrams for $\mathbf{2_{Br\text{-}S}}$ species

reactivity for singlet tetrabromosilylene compared to other species.

Substituent effects on isodesmic reactions

On the basis of the Hoffmann, Schleyer, and Schaefer's statement, a stable species must be resistant to fragmentation, isomerization, etc. [33]. In this study, applying the appropriate isodesmic reactions, we show in detail how the substituent affects on singlet (S) and/or triplet (T) states' stabilities of our divalent molecules, individually. In a theoretical survey on triplet carbenes, Nemirowski and Schreiner stated that the classical π-donor/σ-acceptor substituents such as amino simultaneously stabilizes singlet and destabilizes triplet state [34]. Previously, we revealed that in contradiction of their claim, amino substituents stabilize not only the singlet but also the triplet states [23–25]. Here, using five proposed isodesmic reactions (Scheme 5 and Table 5), we test our previous suggestion for the case of tetrahalosilylenes, at (U)M06-2X/6-311 ++G**.

Isodesmic reaction#1 shows the dehydrogenation of scrutinized silanes by singlet ($\mathbf{1_{H\text{-}S}}$) and/or triplet ($\mathbf{1_{H\text{-}T}}$) reference non-planar carbenes. This reaction describes that the energy change is associated with an exothermic reaction that increases its exothermicity on going from fluorine to bromine and making the $\mathbf{2_{H\text{-}S}}$ silylene as the least stable singlet species ($\Delta E_1 = -142.75$ kJ/mol), and the $\mathbf{2_{H\text{-}T}}$ silylene as the most stable triplet species ($\Delta E_1 = -25.16$ kJ/mol). Accordingly, the highest stability is demonstrated by $\mathbf{2_{Br\text{-}S}}$ ($\Delta E_1 = -200.43$ kJ/mol), and the lowest stability is recognized by $\mathbf{2_{Br\text{-}T}}$ ($\Delta E_1 = +9.53$ kJ/mol). Obviously, every S silylene appears more stable than its corresponding T state for showing a higher ΔE_1. In isodesmic reaction#2, heat of dehydrogenation (ΔE_2) is approximated for S and/or T carbene-like atoms using the parent planar conjugated singlet ($1_{H\text{-}S}$ *) and/or triplet $1_{H\text{-}T}$ * carbenes to examine the mesomeric effects of halogen atoms, along with hyperconjugation effect on stability of silylenes. The higher is the ΔE_2 value, the more is the stability of silylenes. Based on heat of dehydrogenation in this exothermic reaction, the highest stabilization is encountered for $\mathbf{2_{Br\text{-}S}}$ by −302.01 kJ/mol followed by $\mathbf{2_{Cl\text{-}S}}$ (−291.56 kJ/mol), $\mathbf{2_{I\text{-}S}}$ (−280.98 kJ/mol), $\mathbf{2_{F\text{-}S}}$ (−271.87 kJ/mol), to $\mathbf{2_{H\text{-}S}}$ (−262.30 kJ/mol) decreases for the corresponding triplet ones. Also, we estimate relative stability for the studied species employing the $\mathbf{1_{H\text{-}S}}$* and/or $\mathbf{1_{H\text{-}T}}$* planar carbenes and non-planar allene (1_H **) as the references in third isodesmic reaction [35–38]. This reaction indicates that the hyperconjugation of hydrogen atoms has a 333.90 kJ/mol stabilizing effect on $\mathbf{1_{H\text{-}S}}$ and 341.92 kJ/mol on its triplet state ($\mathbf{1_{H\text{-}T}}$). Isodesmic reaction#3 shows that the dehydrogenation is coupled with endothermic reaction which decreases going from planar conjugated $\mathbf{1_{H\text{-}S}^{*}}$ and/or $\mathbf{1_{H\text{-}T}^{*}}$ carbene to its corresponding non-planar analogous and increases going from every S state to its corresponding T state. In isodesmic reaction#4, we estimate relative stability for our scrutinized silylenes using the planar conjugated $\mathbf{1_{H\text{-}S}^{*}}$ and/or $\mathbf{1_{H\text{-}T}^{*}}$ carbene and singlet and/or triplet methylene ($:CH_2$). The results are very different to those obtained from heat of dehydrogenation of Rxn 1–3, indicating stabilization of S carbenes and S silylenes by about 6.3–8.4 kJ/mol more than their corresponding T carbenes and T silylenes, and so carbenes are less stabilized than silylenes. Fascinatingly, the π-donor/σ-acceptor halogen groups stabilize both S and T silylenes. This is related to the higher electronegativity of halogen atoms which makes them as stronger σ-acceptors and henceforth prefers S over T state. Furthermore, on account of the higher electronegativity the π-donating of halogen atoms in S silylenes is higher than that of T analogous. Hydrogen groups stabilize both $\mathbf{1_{H\text{-}S}}$ and $\mathbf{1_{H\text{-}T}}$ carbenes (Table S6). Also, relative stability of $\mathbf{2_{H\text{-}S}}$ and $\mathbf{2_{H\text{-}T}}$ silylenes (Table S6) is more than twice of $\mathbf{1_{H\text{-}S}}$ and $\mathbf{1_{H\text{-}T}}$ carbenes. The lower electronegativity of silicon than carbon atom and the lower electronegativity of iodine than other halogen atoms lead to higher stability of $\mathbf{2_{I\text{-}T}}$ silylene than $\mathbf{1_{H\text{-}T}}$ carbene ($\Delta E_4 = -467.78$ vs. −200.51 kJ/mol). Consequently, isodesmic reaction#5 shows the dehydrogenation of substituted silanes by $\mathbf{2_{H\text{-}S}}$ and $\mathbf{2_{H\text{-}T}}$ reference silylenes and so the lowest stability is shown by $\mathbf{2_{Br\text{-}T}}$ ($\Delta E_5 = 56.89$ kJ/mol, See Rxn 5 in Scheme 5 and Table 5).

Conclusion

In this survey, we have compared and contrasted thermodynamical, geometrical, and kinetical parameters of nine-membered cyclic carbene and its halogenated silylenes including singlet states ($\mathbf{1_{H\text{-}S}}$–$\mathbf{2_{I\text{-}S}}$) and triplets ($\mathbf{1_{H\text{-}T}}$–$\mathbf{2_{I\text{-}T}}$). Except for reference carbene ($\mathbf{1_H}$) which emerges one imaginary vibrational frequency, all of silylenes show real vibrational frequency and appear as boat-shaped minima on their potential energy surfaces, at DFT. The $\mathbf{2_{Br\text{-}S}}$ shows the highest stability indicated by the highest ΔE_{S-T}, ΔH_{S-T}, and ΔG_{S-T}. From a thermodynamic point of view, all calculated ΔE_{S-T}, ΔH_{S-T}, and ΔG_{S-T} parameters appear with positive values, indicating that every singlet silylene is more stable than its corresponding triplet state. Evidently, among calculated singlet silylenes ($\mathbf{2_{H\text{-}S}}$–$\mathbf{2_{I\text{-}S}}$), the most stable species appears to be $\mathbf{2_{Br\text{-}S}}$ which is 172.43 kJ/mol more stable than its corresponding triplet $\mathbf{2_{Br\text{-}T}}$. The overall trend of ΔE_{S-T}, ΔH_{S-T}, and ΔG_{S-T} is: $\mathbf{2_H < 2_F < 2_I < 2_{Cl} < 2_{Br}}$. From a kinetic viewpoint, $\mathbf{2_{Br\text{-}S}}$ shows the highest value of $\Delta E_{HOMO-LUMO}$ (412.61 kJ/mol) which is higher than that of calculated for the parent form of Kira's synthesized silylene (351.79 kJ/mol). Respecting the σ-donor characteristic of the stable silylenes, the highest nucleophilicity, the highest HOMO energy, and the lowest electrophilicity is calculated for

Scheme 5

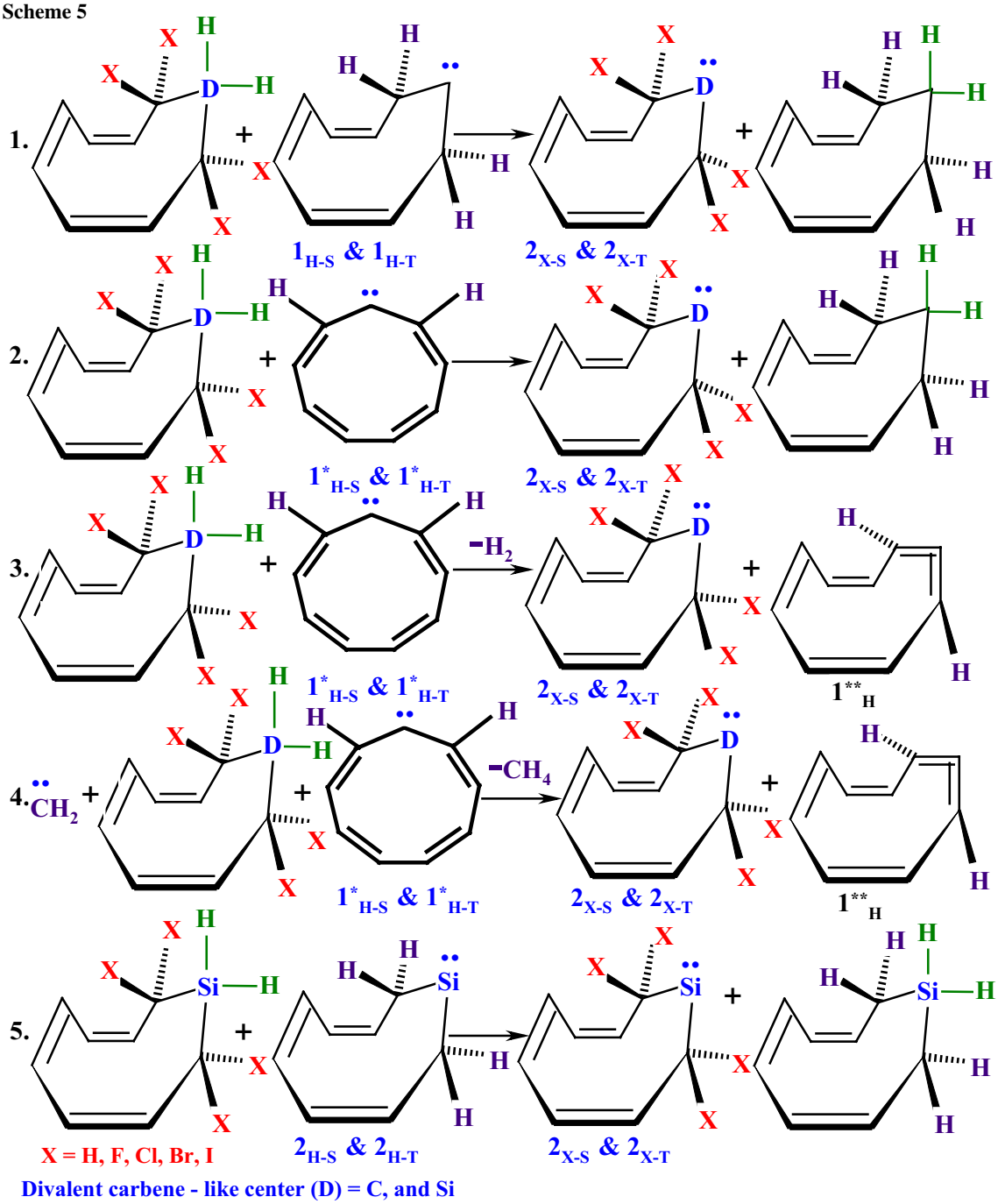

unsubstituted silylene ($\mathbf{2_{H\text{-}S}}$) via hyperconjugation effect. These factors make it theoretically more susceptible for attacking an electrophile. Contrary to our expectation, $\mathbf{2_{H\text{-}S}}$ not only does not turn out to be electrophilic, but also because of its intrinsic angle strain, boat-like structure and hyperconjugation effect turn out as the most nucleophilic character among singlet silylenes. We have employed the NBO analysis to stress the roles of intermolecular donor and acceptor interactions through the second-order perturbation theory. As above the geometrical parameters such as bond length, bond angle, and symmetry compared and contrasted for our silylenes, S silylenes show higher Si–C bond lengths and lower bond angles than their corresponding T states. This is attributed to the intramolecular orbital interactions,

Table 5 The substituent effects on singlet and triplet silylenes (ΔE_1 to ΔE_5, in kJ/mol) via isodesmic reactions 1–5 (see Scheme 5), at (U) M06-2X/6-311++G**

Species	ΔE_1	ΔE_2	ΔE_3	ΔE_4	ΔE_5
$\mathbf{1_{H^-S}}$	0.00	0.00	333.90	−208.54	–
$\mathbf{1_{H^-T}}$	00.00	0.00	341.92	−200.51	–
$\mathbf{2_{H^-S}}$	−142.75	−262.30	71.60	−470.84	− 0.17
$\mathbf{2_{H^-T}}$	−25.16	−42.26	79.63	−462.81	− 0.17
$\mathbf{2_{F^-S}}$	−173.55	−271.87	62.03	−480.41	−9.57
$\mathbf{2_{F^-T}}$	−16.05	−24.70	70.06	−472.38	17.56
$\mathbf{2_{Cl^-S}}$	−188.14	−291.56	71.60	−470.84	0.00
$\mathbf{2_{Cl^-T}}$	0.08	2.93	79.63	-462.81	45.19
$\mathbf{2_{Br^-S}}$	−200.43	−302.01	71.60	−470.84	0.00
$\mathbf{2_{Br^-T}}$	9.53	14.63	79.63	−462.81	56.89
$\mathbf{2_{I^-S}}$	−183.50	−280.98	64.20	−476.06	0.00
$\mathbf{2_{I^-T}}$	−12.08	−15.55	73.78	−467.78	33.94

particularly the interaction of paired electrons on divalent Si atom with $\sigma_{C\alpha\text{-}Br}$* and the interaction of $\sigma_{C\alpha\text{-}Br}$ with $3p_{\pi\,Si}$ orbitals of the molecules. This analysis indicates that there is a negative hyperconjugation between σ^2-bonding orbital of silicon with anti-bonding orbital of carbon-bromine in α,α′-positions of $\mathbf{2_{Br^-S}}$ species which leads to stability of it, and compensating for the mesomeric effect of bromine. Isodesmic reactions are used to assess the effects of substitution on the stability of silylenes. Commonly, it is found that α,α′-tetrahalo groups stabilize both singlet and triplet states of our studied silylenes with a more considerable effect on the singlet. Based on heat of dehydrogenation in exothermic isodesmic reaction, the highest stabilization is encountered for $\mathbf{2_{Br^-S}}$ followed by $\mathbf{2_{Cl^-S}}$, $\mathbf{2_{I^-S}}$, $\mathbf{2_{F^-S}}$, to $\mathbf{2_{H^-S}}$ and decreases for substituted triplet ones. Both singlet and triplet silylenes become differently more stable in the presence of halogen atoms with a more considerable effect on the singlet. Theoretical conclusions are waiting for experimental testing and verifications.

Computational methods

Geometry optimizations of scrutinized silylenes are carried out with the GAMESS program package [39, 40], at the B3LYP [41–45], and M06 [46] methods, with standard triple-zeta 6-311 + G* Pople basis set [47, 48], which is constructive for the explanation of diffuse functions [48, 49], is employed for C, Si, H, F, Cl, and Br atoms, while the valence double-zeta LANL2DZ basis set with effective core potential (ECP) of Hay and Wadt is used for I atom [50]. Dynamics are studied at different methods and levels of accuracy with the DFT outcome expected to provide the more accurate structural and energetic results. For more accurate energetic data, single point calculations are performed at the B3LYP/AUG-cc-pVTZ//B3LYP/6-311 + G* [52], and M06-2X/AUG-cc-pVDZ//M06-2X/6-311 + G* levels. Triplet states are computed using unrestricted broken spin-symmetry UB3LYP and UM06-2X methods at the same levels. The vibrational frequency computations are applied to characterize the nature of stationary points as minimum (NIMAG = 0), or transition state (NIMAG = 1), at B3LYP/6-311++G**//B3LYP/6–311 + G* [51, 52]. The natural bond orbital (NBO) population analysis is calculated at B3LYP/LANL2DZ-6-311++G** and UB3LYP/LANL2DZ-6-311++G** for singlet and triplet states, respectively [53–56]. Also, reactivity is estimated using the same level. Hence, the nucleophilicity index (N) is calculated as $N = E_{HOMO(Nu)} - E_{HOMO(TCNE)}$, where tetracyanoethylene (TCNE) is preferred as Ref. [57–62]. In this scale, the nucleophilicity index for TCNE is $N = 0.0$ eV, presenting the lowest HOMO energy in a long series of organic molecules already considered. This choice allowed us conveniently to handle a nucleophilicity scale of positive values. The capacity of the N index describing the nucleophilic behavior of organic molecules was tested in the context of the analysis of the nucleophilic behavior of a series of captodative ethylenes [57–62]. The global electrophilicity (ω) is computed as $\omega = (\mu^2/2\eta)$ [57–62], where μ is the chemical potential ($\mu = (E_{HOMO} + E_{LUMO})/2$) and η is the chemical hardness ($\eta = (E_{LUMO} - E_{HOMO})/2$) [57–62]. Furthermore, χ is the absolute electronegativity ($\chi = -\mu$) is used to predict the electron transfer direction when the substituted species are formed, S is the global softness ($S = 1/2\eta$), and ΔN_{max} is the maximum electronic charge ($\Delta N_{max} = -\mu/\eta$) [57–62]. The molecular electrostatic potential (MEP) maps are anticipated at B3LYP/AUG-cc-pVTZ.

Acknowledgements This research is financially supported by Technical and Vocational University of Tehran, Dr. Shariaty College, Tehran, and North Tehran Branch, Islamic Azad University, Tehran, Iran.

References

1. Kassaee MZ, Zandi H, Haerizade BN, Ghambarian M (2012) Comput Theor Chem 1001:39
2. Momeni MR, Shakib FA (2011) Organomet 30:5027
3. Ayoubi-Chianeh M, Kassaee MZ, Ashenagar S, Cummings PT (2019) J Phys Org Chem 32:e3956
4. Brück A, Gallego D, Wang W, Irran E, Driess M, Hartwig JF (2012) Angew Chem Int Ed 51:11478
5. Li J, Merkel S, Henn J, Meindl K, Döring A, Roesky HW, Ghadwal RS, Stalke D (2010) Inorg Chem 49:775
6. Yang W, Fu H, Wang H, Chen M, Ding Y, Roesky HW, Jana A (2009) Inorg Chem 48:5058
7. Yamada T, Mawatari A, Tanabe M, Osakada K, Tanase T (2009) Angew Chem 121:576
8. Blom B, Enthaler S, Inoue S, Irran E, Driess M (2013) J Am Chem Soc 135:6703

9. Tan G, Blom B, Gallego D, Driess M (2013) Organometallics 33:363
10. Blom B, Stoelzel M, Driess M (2013) Chem Eur J 19:40
11. Stoelzel M, Präsang C, Blom B, Driess M (2013) Aust J Chem 66:1163
12. Protchenko AV, Birjkumar KH, Dange D, Schwarz AD, Vidovic D, Jones C, Kaltsoyannis N, Mountford P, Aldridge S (2012) J Am Chem Soc 134:6500
13. Rekken BD, Brown TM, Fettinger JC, Tuononen HM, Power PP (2012) J Am Chem Soc 134:6504
14. Asay M, Inoue S, Driess M (2011) Angew Chem Int Ed 50:9589
15. Sasamori T, Tokitoh N (2005) In: King RB (ed) Encyclopedia of Inorganic Chemistry II. Wiley, Chichester, p 1698
16. Slipchenko LV, Krylov AI (2002) J Chem Phys 117:4694
17. Denk M, Lennon R, Hayashi R, West R, Haaland A, Belyakov H, Verne P, Wagner M, Metzler N (1994) J Am Chem Soc 116:2691
18. Gehrhus B, Lappert MF, Heinicke J, Boese R, Bläser D (1995) J Chem Soc Chem Commun 19:1931–1932
19. West R, Denk M (1996) Pure Appl Chem 68:785
20. Heinicke J, Oprea A, Kindermann MK, Karpati T, Nyulaszi L, Veszpremi T, Hitchcock PB, Lappert MF, Maciejewski H (1998) Organometallics 17:5599
21. Kira M, Ishida S, Iwamoto T, Kabuto C (1999) J Am Chem Soc 121:9722
22. Driess M, Yao S, Brym M, Wüllen C, Lentz D (2006) J Am Chem Soc 128:9628
23. Kassaee MZ, Koohi M (2013) J Phys Org Chem 26:540
24. Kassaee MZ, Koohi M, Mohammadi R, Ghavami M (2013) J Phys Org Chem 26:908
25. Koohi M, Kassaee MZ, Haerizade BN, Ghavami M, Ashenagar S (2015) J Phys Org Chem 28:514
26. Naderi F, Bagheri R, Yari M (2013) J Phys Theor Chem 9:281
27. Mekky ABH, Elhaes HG, El-Okr MM, Ibrahim MA (2015) J Nanomater Mol Nanotechnol 4:2
28. Mizuhata Y, Sasamori T, Tokitoh N (2009) Chem Rev 109:3479
29. Govindarajan M, Karabacak M, Suvitha A, Periandy S (2012) Spectrochim Acta A Mol Biomol Spectrosc 89:137
30. Ruiz-Espinoza A, Ramos E, Salcedo R (2013) Comput Theor Chem 1016:36
31. Dheivamalar S, Sugi L, Ambigai K (2016) Comput Chem 4:17
32. Dheivamalar S, Sugi L (2015) Spectrochim Acta A Mol Biomol Spectrosc 151:687
33. Hoffmann R, Schleyer PR, Schaefer HF (2008) Angew Chem Int Ed 47:7164
34. Nemirowski A (2007) Schreiner PR). J Org Chem 72:9533–9540
35. Kassaee MZ, Koohi M (2005) J Mol Struct (THEOCHEM) 755:91
36. Kassaee MZ, Koohi M, Arshadi S (2005) J Mol Struct (THEOCHEM) 724:61
37. Kassaee MZ, Koohi M (2007) J Mol Struct (THEOCHEM) 815:21
38. Kassaee MZ, Koohi M (2007) J Mol Struct (THEOCHEM) 810:53
39. Schmidt MW, Baldridge KK, Boatz JA, Elbert ST, Gordon MS, Jensen JH, Koseki S, Matsunaga N, Nguyen KA, Su SJ, Windus TL, Dupuis M, Montgomery JA (1993) J Comput Chem 14:1347
40. Sobolewski AL, Domcke W (2002) J Phys Chem A 106:4158
41. Becke AD (1988) Phys Rev A 38:3098
42. Becke AD (1993) J Chem Phys 98:5648
43. Becke AD (1996) J Chem Phys 104:1040
44. Lee C, Yang W, Parr RG (1988) Phys Rev B 37:785
45. Krishna R, Frisch MJ, Pople JA (1980) J Chem Phys 72:4244
46. Zhao Y, Truhlar DG (2008) Theor Chem Account 120:215
47. Francl MM, Pietro WJ, Hehre WJ, Binkley JS, Gordon MS, DeFrees DJ, Pople JA (1982) J Chem Phys 77:3654
48. Clark T, Chandrasekhar J, Spitznagel GW, Schleyer PR (1983) J Comput Chem 4:294
49. Frisch MJ, Pople JA, Binkley JS (1984) J Chem Phys 80:3265
50. Schlegel HB, Frisch MJ (1995) Int J Quantum Chem 54:83
51. Kendall RA, Dunning TH Jr, Harrison RJ (1992) J Chem Phys 96:6796
52. Hehre WJ, Radom L, PvR Schleyer, Pople JA (1986) Ab Initio Molecular Orbital Theory. John Wiley & Sons, New York
53. Foresman JB, Frisch A (1996) Exploring Chemistry with Electronic structure Methods. Gaussian Inc, Pittsburgh
54. Glendening ED, Reed AE, Carpenter JE, Weinhold F NBO Version 3.1
55. Weinhold F, Glendening ED, NBO Version 7.0
56. Weinhold F (2012) J Comput Chem 33:2363
57. Glendening ED, Landis CR, Weinhold F (2012) Wiley Interdiscip Rev Comput Mol Sci 2:1
58. Domingo LR, Pérez P (2011) Org Biomol Chem 9:7168
59. Domingo LR, Chamorro E, Pérez P (2008) J Org Chem 73:4615
60. Parr RG, Szentpaly L, Liu S (1999) J Am Chem Soc 121:1922
61. Pearson RG (1989) J Org Chem 54:1423
62. Chattaraj PK, Giri S (2007) J Phys Chem A 111:11116
63. Padmanabhan J, Parthasarathi R, Subramanian V, Chattaraj PK (2007) J Phys Chem A 111:1358